

Observation of $\bar{B}_{(s)}^0 \rightarrow J/\psi f_1(1285)$ Decays and Measurement of the $f_1(1285)$ Mixing Angle

R. Aaij *et al.**

(LHCb Collaboration)

(Received 8 October 2013; published 4 March 2014)

Decays of \bar{B}_s^0 and \bar{B}^0 mesons into $J/\psi \pi^+ \pi^- \pi^+ \pi^-$ final states, produced in pp collisions at the LHC, are investigated using data corresponding to an integrated luminosity of 3 fb^{-1} collected with the LHCb detector. $\bar{B}_{(s)}^0 \rightarrow J/\psi f_1(1285)$ decays are seen for the first time, and the branching fractions are measured. Using these rates, the $f_1(1285)$ mixing angle between strange and nonstrange components of its wave function in the $q\bar{q}$ structure model is determined to be $\pm(24.0_{-2.6}^{+3.1+0.6})^\circ$. Implications on the possible tetraquark nature of the $f_1(1285)$ are discussed.

DOI: 10.1103/PhysRevLett.112.091802

PACS numbers: 14.40.Be, 13.20.He, 13.25.-k, 14.65.Bt

Light flavorless hadrons, f , are not entirely understood as $q\bar{q}$ states. Some states with the same quantum numbers such as the η and η' exhibit mixing [1]. Others, such as the $f_0(500)$ and the $f_0(980)$, could be mixed $q\bar{q}$ states, or they could be comprised of tetraquarks [2]. In addition, some states, such as the $f_0(1500)$, are discussed as being made solely of gluons [3]. Understanding if the f states are indeed explained by the quark model is crucial to identifying other exotic structures. Previous investigations of \bar{B}_s^0 and \bar{B}^0 decays (called generically \bar{B}) into a J/ψ meson and a $\pi^+ \pi^-$ [4,5] or $K^+ K^-$ [6,7] pair have revealed the presence of several light flavorless meson resonances including the $f_0(500)$ and the $f_0(980)$. Use of $\bar{B} \rightarrow J/\psi f$ decays has been suggested as an excellent way of both measuring mixing angles and discerning if some of the f states are tetraquarks [8,9]. In this Letter the $J/\psi \pi^+ \pi^- \pi^+ \pi^-$ final state is investigated with the aim of seeking additional f states. (Mention of a particular process also implies the use of its charge conjugated decay.)

Data are obtained from 3 fb^{-1} of integrated luminosity collected with the LHCb detector [10] using pp collisions. One third of the data was acquired at a center-of-mass energy of 7 TeV, and the remainder at 8 TeV. The LHCb detector is a single-arm forward spectrometer covering the pseudorapidity range $2 < \eta < 5$, designed for the study of particles containing b or c quarks. The detector includes a high precision tracking system consisting of a silicon-strip vertex detector surrounding the pp interaction region, a large-area silicon-strip detector located upstream of a dipole magnet with a bending power of about 4 Tm, and three stations of silicon-strip detectors and straw drift tubes

placed downstream. The combined tracking system provides a momentum measurement with relative uncertainty that varies from 0.4% at 5 GeV to 0.6% at 100 GeV. (We work in units where $c = 1$.) The impact parameter (IP) is defined as the minimum track distance with respect to the primary vertex. For tracks with large transverse momentum, p_T , with respect to the proton beam direction, the IP resolution is approximately $20 \mu\text{m}$. Charged hadrons are identified using two ring-imaging Cherenkov (RICH) detectors. Photon, electron, and hadron candidates are identified by a calorimeter system consisting of scintillating-pad and preshower detectors, an electromagnetic calorimeter, and a hadronic calorimeter. Muons are identified by a system composed of alternating layers of iron and multiwire proportional chambers.

The LHCb trigger [11] consists of a hardware stage, based on information from the calorimeter and muon systems, followed by a software stage that applies event reconstruction. Events selected for this analysis are triggered by a candidate $J/\psi \rightarrow \mu^+ \mu^-$ decay, required to be consistent with coming from the decay of a b hadron by using either IP requirements or detachment from the associated primary vertex. Simulations are performed using PHYTHIA [12] with the specific tuning given in Ref. [13], and the LHCb detector description based on GEANT4 [14] described in Ref. [15]. Decays of b hadrons are based on EVTGEN [16].

Events are preselected and then are further filtered using a multivariate analyzer based on the boosted decision tree (BDT) technique [17]. In the preselection, all charged track candidates are required to have $p_T > 250 \text{ MeV}$, while for muon candidates the requirement is $p_T > 550 \text{ MeV}$. Events must have a $\mu^+ \mu^-$ combination that forms a common vertex with $\chi^2 < 20$, an invariant mass between -48 and $+43 \text{ MeV}$ of the J/ψ meson mass, and are constrained to the J/ψ mass. The four pions must have a vector summed $p_T > 1.0 \text{ GeV}$, form a vertex with $\chi^2 < 50$ for 5 degrees of freedom, and a common vertex with the

* Full author list given at the end of the article.

Published by the American Physical Society under the terms of the Creative Commons Attribution 3.0 License. Further distribution of this work must maintain attribution to the author(s) and the published articles title, journal citation, and DOI.

J/ψ candidate with $\chi^2 < 90$ for 9 degrees of freedom. The angle between the \bar{B} momentum and the vector from the primary vertex to the \bar{B} decay vertex is required to be smaller than 2.56° . Particle identification [18] requirements are based on the difference in the logarithm of the likelihood, $\text{DLL}(h_1 - h_2)$, to distinguish between the hypotheses h_1 and h_2 . We require $\text{DLL}(\pi - \mu) > -10$ and $\text{DLL}(\pi - K) > -10$. We also explicitly eliminate candidate $\psi(2S)[\text{or } X(3872)] \rightarrow J/\psi \pi^+ \pi^-$ events by rejecting any candidate where one $J/\psi \pi^+ \pi^-$ combination is within 23 MeV of the $\psi(2S)$ or 9 MeV of the $X(3872)$ meson masses. Other resonant contributions such as $\bar{B} \rightarrow \psi(4160) \pi^+ \pi^-$ are searched for, but not found.

The BDT uses 12 variables that are chosen to separate signal and background: the minimum $\text{DLL}(\pi - \mu)$ of the μ^+ and μ^- , the scalar p_T sum of the four pions, and the vector p_T sum of the four pions; relating to the \bar{B} candidate: the flight distance, the vertex χ^2 , the p_T , and the χ^2_{IP} , which is defined as the difference in χ^2 of a given primary vertex reconstructed with and without the considered particle. In addition, considering the $\pi^+ \pi^+$ and $\pi^- \pi^-$ as pairs of particles, the minimum p_T , and the minimum χ^2_{IP} of each pair are used. The signal sample used for BDT training is based on simulation, while the background sample uses the sideband 200–250 MeV above the \bar{B}_s^0 mass peak from 1/3 of the available data. The BDT is then tested on independent samples from the same sources. The BDT selection is optimized by taking the signal, S , and background, B , events within ± 20 MeV of the \bar{B}_s^0 peak from the preselection and maximizing $S^2/(S+B)$ by using the signal and background efficiencies provided as a function of BDT.

The $J/\psi \pi^+ \pi^- \pi^+ \pi^-$ invariant mass distribution is shown in Fig. 1. Multiple combinations are at the 6% level and a single candidate is chosen based on vertex χ^2 and J/ψ mass. We fit the mass distribution using the same signal function shape for both \bar{B}_s^0 and \bar{B}^0 peaks. This shape is a double Crystal Ball function [19] with common means and radiative tail parameters obtained from simulation. The combinatorial background is parametrized with an exponential function. There are $1193 \pm 46 \bar{B}_s^0$ and $839 \pm 39 \bar{B}^0$ decays. Possible backgrounds caused by particle misidentification, for example $\bar{B}^0 \rightarrow J/\psi \pi^+ K^- \pi^+ \pi^-$ decays, would appear as signal if the particle identification incorrectly assigns the K^- as a π^- . In this case the invariant mass is always below the \bar{B}^0 signal region. Evaluating all such backgrounds shows negligible contributions in the signal regions. These and other low-mass backgrounds are described by a Gaussian distribution.

In order to improve the four-pion mass resolution we kinematically fit each candidate with the constraints that the $\mu^+ \mu^-$ be at the J/ψ mass and that the $J/\psi \pi^+ \pi^- \pi^+ \pi^-$ be at the \bar{B} mass. The four-pion invariant mass distributions for \bar{B}_s^0 and \bar{B}^0 decays within ± 20 MeV of the \bar{B} mass peaks are shown in Fig. 2. The backgrounds, determined from fits to

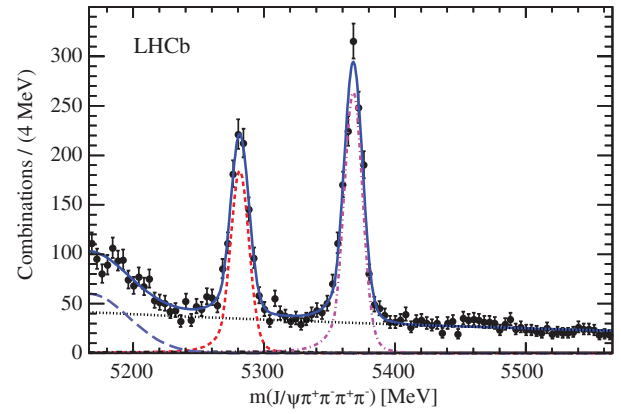


FIG. 1 (color online). Invariant mass distribution for $J/\psi \pi^+ \pi^- \pi^+ \pi^-$ combinations. The data are fit with Crystal Ball functions for \bar{B}^0 [(red) dashed curve] and \bar{B}_s^0 [(purple) dot-dashed curve] signals, an exponential function for combinatoric background (black) dotted curve, and a Gaussian shape for lower mass background (blue) long-dashed curve. The total is shown with a (blue) solid curve.

the number of events in the region 40–80 MeV above the \bar{B}_s^0 mass, are subtracted.

There are clear signals around 1285 MeV in both \bar{B}_s^0 and \bar{B}^0 decays with structures at higher masses. The J/ψ decay angular distribution is used to probe the spin of the recoiling four-pion system. We examine the distribution of the helicity angle θ of the μ^+ with respect to the \bar{B} direction in the J/ψ rest frame, after correcting for the angular acceptance using simulation. The resulting distribution is then fit by the sum of shapes $(1 - \alpha)\sin^2\theta$ and $\alpha(1 + \cos^2\theta)/2$, where α is the fraction of the helicity ± 1 component. For scalar four-pion states the J/ψ helicity is 0, while for higher spin states it is a mixture of helicity 0 and helicity ± 1 components. We also show in Fig. 2 the helicity ± 1 yields. In the region near 1285 MeV there is a significant helicity ± 1 component, as expected if the state we are observing is the $f_1(1285)$.

There is also a large and wider peak near 1450 MeV in the \bar{B}_s^0 channel. Previously we observed a structure at a mass near 1475 MeV using $\bar{B}_s^0 \rightarrow J/\psi \pi^+ \pi^-$ decays that we attributed to $f_0(1370)$ decay. However, it could equally well be the $f_0(1500)$ meson, an interpretation favored by Ochs [3]. While the $f_0(1500)$ is known to decay into four pions, the structure observed in our data cannot be pure spin 0 because of the significant helicity ± 1 component in this mass region. We do not pursue further the composition of the higher mass regions in either \bar{B}_s^0 or \bar{B}^0 decays in this Letter.

We use the measured branching fractions of $\bar{B}_s^0 \rightarrow J/\psi \pi^+ \pi^-$ [4] and $\bar{B}^0 \rightarrow J/\psi \pi^+ \pi^-$ [5] for normalizations. The data selection is updated from that used in previous publications to more closely follow the procedure in this analysis. We find signal yields of $22476 \pm 177 \bar{B}_s^0$ events and $16016 \pm 187 \bar{B}^0$ events within ± 20 MeV of the signal

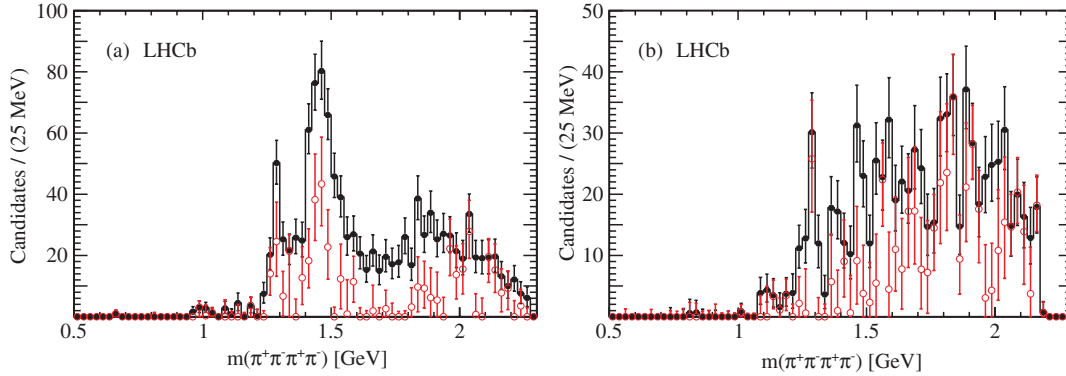


FIG. 2 (color online). Background subtracted invariant mass distributions of the four pions in (a) \bar{B}_s^0 and (b) \bar{B}^0 decays are shown in the histogram overlaid with the (black) solid points with the error bars indicating the uncertainties. The open (red) circles show the helicity ± 1 components of the signals.

peaks. The overall efficiencies determined by simulation are $(1.411 \pm 0.015)\%$ and $(1.317 \pm 0.015)\%$, respectively, for \bar{B}_s^0 and \bar{B}^0 decays, where the uncertainty is statistical only. The relative efficiencies for the J/ψ

$\pi^+\pi^-\pi^+\pi^-$ final states with respect to $J/\psi \pi^+\pi^-$ are 14.3% and 14.5% for \bar{B}_s^0 and \bar{B}^0 decays, with small statistical uncertainties. We compute the overall branching fraction ratios

$$\begin{aligned} \mathcal{B}(\bar{B}_s^0 \rightarrow J/\psi \pi^+ \pi^- \pi^+ \pi^-) / \mathcal{B}(\bar{B}_s^0 \rightarrow J/\psi \pi^+ \pi^-) &= 0.371 \pm 0.015 \pm 0.022, \\ \mathcal{B}(\bar{B}^0 \rightarrow J/\psi \pi^+ \pi^- \pi^+ \pi^-) / \mathcal{B}(\bar{B}^0 \rightarrow J/\psi \pi^+ \pi^-) &= 0.361 \pm 0.017 \pm 0.021. \end{aligned}$$

The systematic uncertainties arise from the decay model (5.0%), background shape (0.8%), signal shape (0.8%), simulation statistics (1.9%), and tracking efficiencies (2.0%), resulting in a total of 5.8%.

We proceed to determine the $J/\psi f_1(1285)$ yields by fitting the individual four-pion mass spectra in both \bar{B}_s^0 and \bar{B}^0 final states. The $f_1(1285)$ state is modeled by a relativistic Breit-Wigner multiplied by phase space and convoluted with our mass resolution of 3 MeV. We take the mass and width of the $f_1(1285)$ as 1282.1 ± 0.6 MeV and 24.2 ± 1.1 MeV, respectively [1]. The combinatorial background is constrained from sideband data and is allowed

to vary by its statistical uncertainty. Backgrounds from higher mass resonances are parametrized by Gaussian shapes whose masses and widths are allowed to vary. We restrict the fits to the interval 1.1–1.5 GeV, which contains 94.3% of the signal. The fits to the data are shown in Fig. 3. The results of the fits are listed in Table I along with twice the negative change in the logarithm of the likelihood ($-2\Delta \ln L$) if fit without the signal, and the resulting signal significance. The systematic uncertainties from the signal shape and higher mass resonances have been included. Both final states are seen with significance above five standard deviations. This constitutes the first observation of the

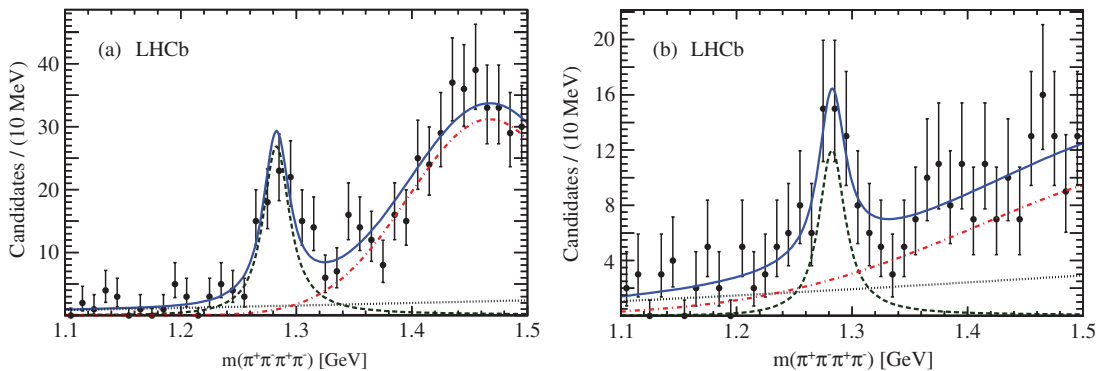


FIG. 3 (color online). Fits to the four-pion invariant mass in (a) \bar{B}_s^0 and (b) \bar{B}^0 decays. The data are shown as points, the signals components as (black) dashed curves, the combinatorial background by (black) dotted curves, and the higher mass resonance tail by (red) dot-dashed curves.

TABLE I. Fit results for $\bar{B}_s^0 \rightarrow J/\psi f_1(1285)$ and $\bar{B}^0 \rightarrow J/\psi f_1(1285)$ decays.

	Yield	$-\Delta \ln L$	Significance (σ)
\bar{B}_s^0	110.2 ± 15.0	58.1	7.2
\bar{B}^0	49.2 ± 11.4	29.5	5.2

$f_1(1285)$ in b -hadron decays. As a consistency check, we also perform a simultaneous fit to both \bar{B}_s^0 and \bar{B}^0 samples letting the mass and width vary in the fit. We find the

$$\frac{\mathcal{B}[\bar{B}_s^0 \rightarrow J/\psi f_1(1285), f_1(1285) \rightarrow \pi^+\pi^-\pi^+\pi^-]}{\mathcal{B}[\bar{B}_s^0 \rightarrow J/\psi \pi^+\pi^-]} = (3.82 \pm 0.52^{+0.29}_{-0.32})\%,$$

$$\frac{\mathcal{B}[\bar{B}^0 \rightarrow J/\psi f_1(1285), f_1(1285) \rightarrow \pi^+\pi^-\pi^+\pi^-]}{\mathcal{B}[\bar{B}^0 \rightarrow J/\psi \pi^+\pi^-]} = (2.32 \pm 0.54 \pm 0.11)\%,$$

$$\frac{\mathcal{B}[\bar{B}^0 \rightarrow J/\psi f_1(1285)]}{\mathcal{B}[\bar{B}_s^0 \rightarrow J/\psi f_1(1285)]} = (11.6 \pm 3.1^{+0.7}_{-0.8})\%.$$

For the latter ratio we use a \bar{B}_s^0/\bar{B}^0 production ratio of 0.259 ± 0.015 [20]; this uncertainty is taken as systematic. The other systematic uncertainties are listed in Table II. The shape of the high-mass tail is changed in the case of \bar{B}_s^0 decays from a single Gaussian to two relativistic Breit-Wigner shapes corresponding to the mass and width values of the $f_1(1420)$ and the $f_0(1500)$ mesons. For the \bar{B}^0 high mass shape we change from a Gaussian shape to a second order polynomial. The decay model reflects the allowed variation in the fraction of $\rho^0\rho^0$ and $\rho^0\pi^+\pi^-$ decays. The total uncertainties are ascertained by adding the individual components in quadrature separately for the positive and negative values.

Considering the $f_1(1285)$ as a mixed $q\bar{q}$ state, we characterize the mixing with a 2×2 rotation matrix containing a single parameter, the angle ϕ , so that the wave functions of the $f_1(1285)$ and its partner, indicated by f_1^* , are given by

$$|f_1(1285)\rangle = \cos\phi|n\bar{n}\rangle - \sin\phi|s\bar{s}\rangle,$$

$$|f_1^*\rangle = \sin\phi|n\bar{n}\rangle + \cos\phi|s\bar{s}\rangle,$$

$$\text{where } |n\bar{n}\rangle \equiv \frac{1}{\sqrt{2}}(|u\bar{u}\rangle + |d\bar{d}\rangle).$$
 (1)

The decay widths can be written as [8]

$$\Gamma(\bar{B}^0 \rightarrow J/\psi f_1(1285)) = 0.5|A_0|^2|V_{cd}|^2\Phi_0\cos^2\phi,$$

$$\Gamma(\bar{B}_s^0 \rightarrow J/\psi f_1(1285)) = |A_s|^2|V_{cs}|^2\Phi_s\sin^2\phi,$$
 (2)

where A_i is the tree level amplitude, V_{cd} and V_{cs} are quark mixing matrix elements, and Φ_i are phase space factors. The amplitude ratio $|A_0|/|A_s|$ is taken as unity [8]. The width ratio is given by

$$\frac{\mathcal{B}[\bar{B}^0 \rightarrow J/\psi f_1(1285)]}{\mathcal{B}[\bar{B}_s^0 \rightarrow J/\psi f_1(1285)]} = \frac{\tau_0}{2\tau_s} \frac{|V_{cd}|^2\Phi_0\cos^2\phi}{|V_{cs}|^2\Phi_s\sin^2\phi},$$
 (3)

where τ_s is the \bar{B}_s^0 lifetime and τ_0 is the \bar{B}^0 lifetime. The angle ϕ is then given by

$$\tan^2\phi = \frac{1}{2} \frac{\mathcal{B}[\bar{B}_s^0 \rightarrow J/\psi f_1(1285)]}{\mathcal{B}[\bar{B}^0 \rightarrow J/\psi f_1(1285)]} \frac{\tau_0}{\tau_s} \frac{|V_{cd}|^2\Phi_0}{|V_{cs}|^2\Phi_s}$$

$$= 0.1970 \pm 0.053^{+0.014}_{-0.012}.$$
 (4)

The ratio of the phase space factors Φ_0/Φ_s equals 0.855. The other input values are $\tau_s = 1.508$ ps [21], $\tau_0 = 1.519$ ps, $|V_{cd}| = 0.2245$, and $|V_{cs}| = 0.97345$ [1]. We use the lifetime measured in $\bar{B}_s^0 \rightarrow J/\psi\phi$ decays as the helicity components are in approximately the same ratio as in $J/\psi f_1(1285)$. No uncertainties are assigned on these

TABLE II. Systematic uncertainties of the branching fractions $\mathcal{B}[\bar{B} \rightarrow J/\psi f_1(1285), f_1(1285) \rightarrow \pi^+\pi^-\pi^+\pi^-]$ and the \bar{B}^0/\bar{B}_s^0 rate ratio. The “+” and “-” signs indicate the positive and negative uncertainties, respectively. All numbers are in (%).

Source	\bar{B}^0		\bar{B}_s^0		Ratio	
	+	-	+	-	+	-
Mass and width of f_1	2.0	2.0	2.7	2.7	1.5	1.5
Shape of high mass	0.6	0	0	3.7	0	3.8
Efficiency	2.0	2.0	2.0	2.0	0	0
Tracking	2.0	2.0	2.0	2.0	0	0
Simulation statistics	2.0	2.0	2.0	2.0	0	0
Total	4.0	4.0	4.4	5.7	1.5	4.1

TABLE III. Branching fractions used for normalization.

Rate	Value	Ref.
$\mathcal{B}(\bar{B}_s^0 \rightarrow J/\psi \pi^+ \pi^-) / \mathcal{B}(\bar{B}_s^0 \rightarrow J/\psi \phi)$	$(19.79 \pm 0.47 \pm 0.52)\%$	[4]
$\mathcal{B}(\bar{B}^0 \rightarrow J/\psi \pi^+ \pi^-)$	$(3.97 \pm 0.09 \pm 0.11 \pm 0.16) \times 10^{-5}$	[5]
$\mathcal{B}(\bar{B}_s^0 \rightarrow J/\psi \phi)$	$(10.50 \pm 0.13 \pm 0.64 \pm 0.82) \times 10^{-4}$	[6]
$\mathcal{B}(B^- \rightarrow J/\psi K^-)$	$(10.18 \pm 0.42) \times 10^{-4}$	[6]

quantities as they are much smaller than the other errors. The resulting mixing angle is

$$\varphi = \pm(24.0_{-2.6-0.8}^{+3.1+0.6})^\circ.$$

The systematic uncertainty is computed from the systematic errors assigned to the branching fractions.

The $f_1(1285)$ mixing angle has been estimated assuming that it is mixed with the $f_1(1420)$ state. Yang finds $\varphi = \pm(15.8_{-4.6}^{+4.5})^\circ$ using radiative decays [22], consistent with an earlier determination of $\pm(15_{-10}^{+5})^\circ$ [23]. A lattice QCD analysis gives $(31 \pm 2)^\circ$, while another phenomenological calculation gives a range between $(20-30)^\circ$ [24]; see also Ref. [25] for other theoretical predictions. In this analysis we do not specify the other mixed partner.

If the $f_1(1285)$ is a tetraquark state its wave function would be $|f_1\rangle = (1/\sqrt{2})([su][\bar{s}\bar{u}] + [sd][\bar{s}\bar{d}])$ in order for

it to be produced significantly in both \bar{B}_s^0 and \bar{B}^0 decays into $J/\psi f_1(1285)$. Using this wave function, the tetraquark model described in Ref. [8] predicts

$$\frac{\mathcal{B}[\bar{B}^0 \rightarrow J/\psi f_1(1285)]}{\mathcal{B}[\bar{B}_s^0 \rightarrow J/\psi f_1(1285)]} = \frac{1}{4} \frac{\tau_0 |V_{cd}|^2 \Phi_0}{\tau_s |V_{cs}|^2 \Phi_s} = 1.14\%, \quad (5)$$

with small uncertainties. Our measurement of this ratio of $(11.6 \pm 3.1_{-0.8}^{+0.7})\%$ differs by 3.3 standard deviations from the tetraquark interpretation including the systematic uncertainty.

Branching fraction ratios are converted into branching fractions using the previously measured rates listed in Table III. We correct the \bar{B}_s^0 rates to reflect the updated value of the \bar{B}_s^0 to \bar{B}^0 production fraction of 0.259 ± 0.015 [20]. We determine

$$\begin{aligned} \mathcal{B}(\bar{B}_s^0 \rightarrow J/\psi \pi^+ \pi^- \pi^+ \pi^-) &= (7.62 \pm 0.36 \pm 0.64 \pm 0.42) \times 10^{-5}, \\ \mathcal{B}(\bar{B}^0 \rightarrow J/\psi \pi^+ \pi^- \pi^+ \pi^-) &= (1.43 \pm 0.08 \pm 0.09 \pm 0.06) \times 10^{-5}, \end{aligned}$$

where the first uncertainty is statistical, the second and third are systematic, being due to the relative branching fraction measurements and the errors in the absolute branching fraction normalization, respectively. For the \bar{B}_s^0 decay this normalization error is due to the uncertainty on the production ratio of \bar{B}_s^0 versus \bar{B}^0 and is 5.8% [5]. For the

\bar{B}^0 mode the uncertainty is due to the error of 4.1% on $\mathcal{B}(B^- \rightarrow J/\psi K^-)$ [6].

In conclusion, we report the first observations of \bar{B}^0 and $\bar{B}_s^0 \rightarrow J/\psi f_1(1285)$ decays. These are also the first observations of the $f_1(1285)$ meson in heavy quark decays. We determine

$$\begin{aligned} \mathcal{B}[\bar{B}_s^0 \rightarrow J/\psi f_1(1285), \quad f_1(1285) \rightarrow \pi^+ \pi^- \pi^+ \pi^-] &= (7.85 \pm 1.09_{-0.90}^{+0.76} \pm 0.46) \times 10^{-6}, \\ \mathcal{B}[\bar{B}^0 \rightarrow J/\psi f_1(1285), \quad f_1(1285) \rightarrow \pi^+ \pi^- \pi^+ \pi^-] &= (9.21 \pm 2.14 \pm 0.52 \pm 0.38) \times 10^{-7}, \\ \mathcal{B}[\bar{B}_s^0 \rightarrow J/\psi f_1(1285)] &= (7.14 \pm 0.99_{-0.91}^{+0.83} \pm 0.41) \times 10^{-5}, \\ \mathcal{B}[\bar{B}^0 \rightarrow J/\psi f_1(1285)] &= (8.37 \pm 1.95_{-0.66}^{+0.71} \pm 0.35) \times 10^{-6}, \end{aligned}$$

where we use the known branching fraction $\mathcal{B}[f_1(1285) \rightarrow \pi^+ \pi^- \pi^+ \pi^-] = (11.0_{-0.6}^{+0.7})\%$ [1]. Investigation of \bar{B}_s^0 and \bar{B}^0 decays into $J/\psi \pi^+ \pi^- \pi^+ \pi^-$ has revealed the presence of the $J/\psi f_1(1285)$ state in both decay channels. This allows determination of the $f_1(1285)$ mixing angle to be $\pm(24.0_{-2.6-0.8}^{+3.1+0.6})^\circ$, even though the mixing companion of this state is not detected. According to Ref. [8], our measured value disfavors the interpretation of the $f_1(1285)$ as a tetraquark state.

We express our gratitude to our colleagues in the CERN accelerator departments for the excellent performance of the LHC. We thank the technical and administrative staff at the LHCb institutes. We acknowledge support from CERN and from the national agencies CAPES, CNPq, FAPERJ, and FINEP (Brazil); NSFC (China); CNRS/IN2P3 and Region Auvergne (France); BMBF, DFG, HGF, and MPG (Germany); SFI (Ireland); INFN (Italy); FOM and NWO (Netherlands); SCSR (Poland); MEN/IFA (Romania);

MinES, Rosatom, RFBR, and NRC “Kurchatov Institute” (Russia); MinECo, XuntaGal and GENCAT (Spain); SNSF and SER (Switzerland); NAS Ukraine (Ukraine); STFC (United Kingdom); NSF (USA). We also acknowledge the support received from the ERC under FP7. The Tier1 computing centres are supported by IN2P3 (France), KIT, and BMBF (Germany), INFN (Italy), NWO, and SURF (Netherlands), PIC (Spain), GridPP (United Kingdom). We are thankful for the computing resources put at our disposal by Yandex LLC (Russia), as well as to the communities behind the multiple open source software packages that we depend on.

-
- [1] J. Beringer *et al.* (Particle Data Group), *Phys. Rev. D* **86**, 010001 (2012).
- [2] A. H. Fariborz, R. Jora, and J. Schechter, *Phys. Rev. D* **79**, 074014 (2009); S. Weinberg, *Phys. Rev. Lett.* **110**, 261601 (2013); G. 't Hooft, G. Isidori, L. Maiani, A. D. Polosa, and V. Riquer, *Phys. Lett. B* **662**, 424 (2008); N. N. Achasov and A. V. Kiselev, *Phys. Rev. D* **86**, 114010 (2012).
- [3] W. Ochs, *J. Phys. G* **40** (2013) 043001; R. L. Jaffe, *Phys. Rev. D* **15**, 267 (1977).
- [4] R. Aaij *et al.* (LHCb Collaboration), *Phys. Rev. D* **86**, 052006 (2012).
- [5] R. Aaij *et al.* (LHCb Collaboration), *Phys. Rev. D* **87**, 052001 (2013).
- [6] R. Aaij *et al.* (LHCb Collaboration), *Phys. Rev. D* **87**, 072004 (2013).
- [7] R. Aaij *et al.* (LHCb Collaboration), *Phys. Rev. D* **88**, 072005 (2013).
- [8] S. Stone and L. Zhang, *Phys. Rev. Lett.* **111**, 062001 (2013).
- [9] R. Fleischer, R. Knejiens, and G. Ricciardi, *Eur. Phys. J. C* **71**, 1832 (2011); **71**, 1798 (2011).
- [10] A. A. Alves, Jr. *et al.* (LHCb Collaboration), *JINST* **3**, S08005 (2008).
- [11] R. Aaij *et al.*, *JINST* **8**, P04022 (2013).
- [12] T. Sjostrand, S. Mrenna, and P. Z. Skands, *J. High Energy Phys.* **05** 2006 (026).
- [13] I. Belyaev *et al.*, *Nuclear Science Symposium Conference Record (NSS/MIC)* (IEEE, Bellingham, WA, 2010), p. 1155.
- [14] J. Allison *et al.* (GEANT4 Collaboration), *IEEE Trans. Nucl. Sci.* **53**, 270 (2006); S. Agostinelli *et al.* (GEANT4 Collaboration), *Nucl. Instrum. Methods Phys. Res., Sect. A* **506**, 250 (2003).
- [15] M. Clemencic, G. Corti, S. Easo, C. R. Jones, S. Miglioranza, M. Pappagallo, and P. Robbe, *J. Phys. Conf. Ser.* **331**, 032023 (2011).
- [16] D. Lange, *Nucl. Instrum. Methods Phys. Res., Sect. A* **462**, 152 (2001).
- [17] L. Breiman, J. H. Friedman, R. A. Olshen, and C. J. Stone, *Classification and Regression Trees*, (Wadsworth Intl. Group, Belmont, CA, 1984).
- [18] M. Adinolfi *et al.*, *Eur. Phys. J. C* **73**, 2431 (2013).
- [19] T. Skwarnicki, PhD thesis, Institute of Nuclear Physics, Krakow, 1986, DESY-F31-86-02.
- [20] LHCb Collaboration, LHCb-CONF-2013-011; R. Aaij *et al.* (LHCb Collaboration), *J. High Energy Phys.* **04** (2013) 001.
- [21] R. Aaij *et al.* (LHCb Collaboration), *Phys. Rev. D* **87**, 112010 (2013).
- [22] K.-C. Yang, *Phys. Rev. D* **84**, 034035 (2011).
- [23] G. Gidal *et al.*, *Phys. Rev. Lett.* **59**, 2012 (1987).
- [24] J. J. Dudek, R. G. Edwards, B. Joó, M. J. Peardon, D. G. Richards, and C. E. Thomas, *Phys. Rev. D* **83**, 111502 (2011); F. E. Close and A. Kirk, *Z. Phys. C* **76**, 469 (1997).
- [25] D.-M. Li, H. Yu, and Q.-X. Shen, *Chin. Phys. Lett.* **17**, 558 (2000); H.-Y. Cheng, *Phys. Lett. B* **707**, 116 (2012).

R. Aaij,⁴⁰ B. Adeva,³⁶ M. Adinolfi,⁴⁵ C. Adrover,⁶ A. Affolder,⁵¹ Z. Ajaltouni,⁵ J. Albrecht,⁹ F. Alessio,³⁷ M. Alexander,⁵⁰ S. Ali,⁴⁰ G. Alkhazov,²⁹ P. Alvarez Cartelle,³⁶ A. A. Alves Jr.,²⁴ S. Amato,² S. Amerio,²¹ Y. Amhis,⁷ L. Anderlini,^{17,f} J. Anderson,³⁹ R. Andreassen,⁵⁶ M. Andreotti,^{16,e} J. E. Andrews,⁵⁷ R. B. Appleby,⁵³ O. Aquines Gutierrez,¹⁰ F. Archilli,¹⁸ A. Artamonov,³⁴ M. Artuso,⁵⁸ E. Aslanides,⁶ G. Auriemma,^{24,m} M. Baalouch,⁵ S. Bachmann,¹¹ J. J. Back,⁴⁷ A. Badalov,³⁵ C. Baesso,⁵⁹ V. Balagura,³⁰ W. Baldini,¹⁶ R. J. Barlow,⁵³ C. Barschel,³⁷ S. Barsuk,⁷ W. Barter,⁴⁶ V. Batozskaya,²⁷ T. Bauer,⁴⁰ A. Bay,³⁸ J. Beddow,⁵⁰ F. Bedeschi,²² I. Bediaga,¹ S. Belogurov,³⁰ K. Belous,³⁴ I. Belyaev,³⁰ E. Ben-Haim,⁸ G. Bencivenni,¹⁸ S. Benson,⁴⁹ J. Benton,⁴⁵ A. Berezhnoy,³¹ R. Bernet,³⁹ M.-O. Bettler,⁴⁶ M. van Beuzekom,⁴⁰ A. Bien,¹¹ S. Bifani,⁴⁴ T. Bird,⁵³ A. Bizzeti,^{17,h} P. M. Bjørnstad,⁵³ T. Blake,³⁷ F. Blanc,³⁸ J. Blouw,¹⁰ S. Blusk,⁵⁸ V. Bocci,²⁴ A. Bondar,³³ N. Bondar,²⁹ W. Bonivento,¹⁵ S. Borghi,⁵³ A. Borgia,⁵⁸ T. J. V. Bowcock,⁵¹ E. Bowen,³⁹ C. Bozzi,¹⁶ T. Brambach,⁹ J. van den Brand,⁴¹ J. Bressieux,³⁸ D. Brett,⁵³ M. Britsch,¹⁰ T. Britton,⁵⁸ N. H. Brook,⁴⁵ H. Brown,⁵¹ A. Bursche,³⁹ G. Busetto,^{21,q} J. Buytaert,³⁷ S. Cadetdu,¹⁵ R. Calabrese,^{16,e} O. Callot,⁷ M. Calvi,^{20,j} M. Calvo Gomez,^{35,n} A. Camboni,³⁵ P. Campana,^{18,37} D. Campora Perez,³⁷ A. Carbone,^{14,c} G. Carboni,^{23,k} R. Cardinale,^{19,i} A. Cardini,¹⁵ H. Carranza-Mejia,⁴⁹ L. Carson,⁵² K. Carvalho Akiba,² G. Casse,⁵¹ L. Castillo Garcia,³⁷ M. Cattaneo,³⁷ C. Cauet,⁹ R. Cenci,⁵⁷ M. Charles,⁵⁴ P. Charpentier,³⁷ S.-F. Cheung,⁵⁴ N. Chiapolini,³⁹ M. Chrzasczcz,^{39,25} K. Ciba,³⁷ X. Cid Vidal,³⁷ G. Ciezarek,⁵² P. E. L. Clarke,⁴⁹ M. Clemencic,³⁷ H. V. Cliff,⁴⁶ J. Closier,³⁷ C. Coca,²⁸ V. Coco,⁴⁰ J. Cogan,⁶ E. Cogneras,⁵ P. Collins,³⁷ A. Comerma-Montells,³⁵ A. Contu,^{15,37} A. Cook,⁴⁵ M. Coombes,⁴⁵ S. Coquereau,⁸ G. Corti,³⁷ B. Couturier,³⁷ G. A. Cowan,⁴⁹

D. C. Craik,⁴⁷ M. Cruz Torres,⁵⁹ S. Cunliffe,⁵² R. Currie,⁴⁹ C. D' Ambrosio,³⁷ P. David,⁸ P. N. Y. David,⁴⁰ A. Davis,⁵⁶ I. De Bonis,⁴ K. De Bruyn,⁴⁰ S. De Capua,⁵³ M. De Cian,¹¹ J. M. De Miranda,¹ L. De Paula,² W. De Silva,⁵⁶ P. De Simone,¹⁸ D. Decamp,⁴ M. Deckenhoff,⁹ L. Del Buono,⁸ N. Déléage,⁴ D. Derkach,⁵⁴ O. Deschamps,⁵ F. Dettori,⁴¹ A. Di Canto,¹¹ H. Dijkstra,³⁷ M. Dogaru,²⁸ S. Donleavy,⁵¹ F. Dordei,¹¹ A. Dosil Suárez,³⁶ D. Dossett,⁴⁷ A. Dovbnya,⁴² F. Dupertuis,³⁸ P. Durante,³⁷ R. Dzhelyadin,³⁴ A. Dziurda,²⁵ A. Dzyuba,²⁹ S. Easo,⁴⁸ U. Egede,⁵² V. Egorychev,³⁰ S. Eidelman,³³ D. van Eijk,⁴⁰ S. Eisenhardt,⁴⁹ U. Eitschberger,⁹ R. Ekelhof,⁹ L. Eklund,^{50,37} I. El Rifai,⁵ C. Elsasser,³⁹ A. Falabella,^{14,e} C. Färber,¹¹ C. Farinelli,⁴⁰ S. Farry,⁵¹ D. Ferguson,⁴⁹ V. Fernandez Albor,³⁶ F. Ferreira Rodrigues,¹ M. Ferro-Luzzi,³⁷ S. Filippov,³² M. Fiore,^{16,e} M. Fiorini,^{16,e} C. Fitzpatrick,³⁷ M. Fontana,¹⁰ F. Fontanelli,^{19,i} R. Forty,³⁷ O. Francisco,² M. Frank,³⁷ C. Frei,³⁷ M. Frosini,^{17,37,f} E. Furfaro,^{23,k} A. Gallas Torreira,³⁶ D. Galli,^{14,c} M. Gandelman,² P. Gandini,⁵⁸ Y. Gao,³ J. Garofoli,⁵⁸ P. Garosi,⁵³ J. Garra Tico,⁴⁶ L. Garrido,³⁵ C. Gaspar,³⁷ R. Gauld,⁵⁴ E. Gersabeck,¹¹ M. Gersabeck,⁵³ T. Gershon,⁴⁷ P. Ghez,⁴ V. Gibson,⁴⁶ L. Giubega,²⁸ V. V. Gligorov,³⁷ C. Göbel,⁵⁹ D. Golubkov,³⁰ A. Golutvin,^{52,30,37} A. Gomes,² P. Gorbounov,^{30,37} H. Gordon,³⁷ M. Grabalosa Gándara,⁵ R. Graciani Diaz,³⁵ L. A. Granado Cardoso,³⁷ E. Graugés,³⁵ G. Graziani,¹⁷ A. Greco,²⁸ E. Greening,⁵⁴ S. Gregson,⁴⁶ P. Griffith,⁴⁴ L. Grillo,¹¹ O. Grünberg,⁶⁰ B. Gui,⁵⁸ E. Gushchin,³² Y. Guz,^{34,37} T. Gys,³⁷ C. Hadjivasiliou,⁵⁸ G. Haefeli,³⁸ C. Haen,³⁷ T. W. Hafkenscheid,⁶¹ S. C. Haines,⁴⁶ S. Hall,⁵² B. Hamilton,⁵⁷ T. Hampson,⁴⁵ S. Hansmann-Menzemer,¹¹ N. Harnew,⁵⁴ S. T. Harnew,⁴⁵ J. Harrison,⁵³ T. Hartmann,⁶⁰ J. He,³⁷ T. Head,³⁷ V. Heijne,⁴⁰ K. Hennessy,⁵¹ P. Henrard,⁵ J. A. Hernando Morata,³⁶ E. van Herwijnen,³⁷ M. Heß,⁶⁰ A. Hicheur,¹ E. Hicks,⁵¹ D. Hill,⁵⁴ M. Hoballah,⁵ C. Hombach,⁵³ W. Hulsbergen,⁴⁰ P. Hunt,⁵⁴ T. Huse,⁵¹ N. Hussain,⁵⁴ D. Hutchcroft,⁵¹ D. Hynds,⁵⁰ V. Iakovenko,⁴³ M. Idzik,²⁶ P. Ilten,¹² R. Jacobsson,³⁷ A. Jaeger,¹¹ E. Jans,⁴⁰ P. Jatón,³⁸ A. Jawahery,⁵⁷ F. Jing,³ M. John,⁵⁴ D. Johnson,⁵⁴ C. R. Jones,⁴⁶ C. Joram,³⁷ B. Jost,³⁷ M. Kaballo,⁹ S. Kandybei,⁴² W. Kalso,⁶ M. Karacson,³⁷ T. M. Karbach,³⁷ I. R. Kenyon,⁴⁴ T. Ketel,⁴¹ B. Khanji,²⁰ O. Kochebina,⁷ I. Komarov,³⁸ R. F. Koopman,⁴¹ P. Koppenburg,⁴⁰ M. Korolev,³¹ A. Kozlinskiy,⁴⁰ L. Kravchuk,³² K. Kreplin,¹¹ M. Kreps,⁴⁷ G. Krocker,¹¹ P. Krokovny,³³ F. Kruse,⁹ M. Kucharczyk,^{20,25,37,j} V. Kudryavtsev,³³ K. Kurek,²⁷ T. Kvaratskheliya,^{30,37} V. N. La Thi,³⁸ D. Lacarrere,³⁷ G. Lafferty,⁵³ A. Lai,¹⁵ D. Lambert,⁴⁹ R. W. Lambert,⁴¹ E. Lanciotti,³⁷ G. Lanfranchi,¹⁸ C. Langenbruch,³⁷ T. Latham,⁴⁷ C. Lazzeroni,⁴⁴ R. Le Gac,⁶ J. van Leerdam,⁴⁰ J.-P. Lees,⁴ R. Lefèvre,⁵ A. Leflat,³¹ J. Lefrançois,⁷ S. Leo,²² O. Leroy,⁶ T. Lesiak,²⁵ B. Leverington,¹¹ Y. Li,³ L. Li Gioi,⁵ M. Liles,⁵¹ R. Lindner,³⁷ C. Linn,¹¹ B. Liu,³ G. Liu,³⁷ S. Lohn,³⁷ I. Longstaff,⁵⁰ J. H. Lopes,² N. Lopez-March,³⁸ H. Lu,³ D. Lucchesi,^{21,q} J. Luisier,³⁸ H. Luo,⁴⁹ E. Luppi,^{16,e} O. Lupton,⁵⁴ F. Machefert,⁷ I. V. Machikhiliyan,³⁰ F. Maciuc,²⁸ O. Maev,^{29,37} S. Malde,⁵⁴ G. Manca,^{15,d} G. Mancinelli,⁶ J. Maratas,⁵ U. Marconi,¹⁴ P. Marino,^{22,s} R. Märki,³⁸ J. Marks,¹¹ G. Martellotti,²⁴ A. Martens,⁸ A. Martín Sánchez,⁷ M. Martinelli,⁴⁰ D. Martinez Santos,^{41,37} D. Martins Tostes,² A. Martynov,³¹ A. Massafferri,¹ R. Matev,³⁷ Z. Mathe,³⁷ C. Matteuzzi,²⁰ E. Maurice,⁶ A. Mazurov,^{16,37,e} M. McCann,⁵² J. McCarthy,⁴⁴ A. McNab,⁵³ R. McNulty,¹² B. McSkelly,⁵¹ B. Meadows,^{56,54} F. Meier,⁹ M. Meissner,¹¹ M. Merk,⁴⁰ D. A. Milanes,⁸ M.-N. Minard,⁴ J. Molina Rodriguez,⁵⁹ S. Monteil,⁵ D. Moran,⁵³ P. Morawski,²⁵ A. Mordà,⁶ M. J. Morello,^{22,s} R. Mountain,⁵⁸ I. Mous,⁴⁰ F. Muheim,⁴⁹ K. Müller,³⁹ R. Muresan,²⁸ B. Muryn,²⁶ B. Muster,³⁸ P. Naik,⁴⁵ T. Nakada,³⁸ R. Nandakumar,⁴⁸ I. Nasteva,¹ M. Needham,⁴⁹ S. Neubert,³⁷ N. Neufeld,³⁷ A. D. Nguyen,³⁸ T. D. Nguyen,³⁸ C. Nguyen-Mau,^{38,o} M. Nicol,⁷ V. Niess,⁵ R. Niet,⁹ N. Nikitin,³¹ T. Nikodem,¹¹ A. Nomerotski,⁵⁴ A. Novoselov,³⁴ A. Oblakowska-Mucha,²⁶ V. Obraztsov,³⁴ S. Oggero,⁴⁰ S. Ogilvy,⁵⁰ O. Okhrimenko,⁴³ R. Oldeman,^{15,d} G. Onderwater,⁶¹ M. Orlandea,²⁸ J. M. Otalora Goicochea,² P. Owen,⁵² A. Oyanguren,³⁵ B. K. Pal,⁵⁸ A. Palano,^{13,b} M. Palutan,¹⁸ J. Panman,³⁷ A. Papanestis,⁴⁸ M. Pappagallo,⁵⁰ C. Parkes,⁵³ C. J. Parkinson,⁵² G. Passaleva,¹⁷ G. D. Patel,⁵¹ M. Patel,⁵² G. N. Patrick,⁴⁸ C. Patrignani,^{19,i} C. Pavel-Nicorescu,²⁸ A. Pazos Alvarez,³⁶ A. Pearce,⁵³ A. Pellegrino,⁴⁰ G. Penso,^{24,l} M. Pepe Altarelli,³⁷ S. Perazzini,^{14,c} E. Perez Trigo,³⁶ A. Pérez-Calero Yzquierdo,³⁵ P. Perret,⁵ M. Perrin-Terrin,⁶ L. Pescatore,⁴⁴ E. Pesen,⁶² G. Pessina,²⁰ K. Petridis,⁵² A. Petrolini,^{19,i} A. Phan,⁵⁸ E. Picatoste Olloqui,³⁵ B. Pietrzyk,⁴ T. Pilař,⁴⁷ D. Pinci,²⁴ S. Playfer,⁴⁹ M. Plo Casasus,³⁶ F. Polci,⁸ G. Polok,²⁵ A. Poluektov,^{47,33} E. Polycarpo,² A. Popov,³⁴ D. Popov,¹⁰ B. Popovici,²⁸ C. Potterat,³⁵ A. Powell,⁵⁴ J. Prisciandaro,³⁸ A. Pritchard,⁵¹ C. Prouve,⁷ V. Pugatch,⁴³ A. Puig Navarro,³⁸ G. Punzi,^{22,r} W. Qian,⁴ B. Rachwal,²⁵ J. H. Rademacker,⁴⁵ B. Rakotomiramanana,³⁸ M. S. Rangel,² I. Raniuk,⁴² N. Rauschmayr,³⁷ G. Raven,⁴¹ S. Redford,⁵⁴ S. Reichert,⁵³ M. M. Reid,⁴⁷ A. C. dos Reis,¹ S. Ricciardi,⁴⁸ A. Richards,⁵² K. Rinnert,⁵¹ V. Rives Molina,³⁵ D. A. Roa Romero,⁵ P. Robbe,⁷ D. A. Roberts,⁵⁷ A. B. Rodrigues,¹ E. Rodrigues,⁵³ P. Rodriguez Perez,³⁶ S. Roiser,³⁷ V. Romanovsky,³⁴ A. Romero Vidal,³⁶ M. Rotondo,²¹ J. Rouvinet,³⁸ T. Ruf,³⁷ F. Ruffini,²² H. Ruiz,³⁵ P. Ruiz Valls,³⁵ G. Sabatino,^{24,k} J. J. Saborido Silva,³⁶ N. Sagidova,²⁹ P. Sail,⁵⁰ B. Saitta,^{15,d} V. Salustino Guimaraes,² B. Sanmartin Sedes,³⁶ R. Santacesaria,²⁴ C. Santamarina Rios,³⁶ E. Santovetti,^{23,k} M. Sapunov,⁶ A. Sarti,¹⁸ C. Satriano,^{24,m} A. Satta,²³ M. Savrie,^{16,e} D. Savrina,^{30,31} M. Schiller,⁴¹ H. Schindler,³⁷ M. Schlupp,⁹ M. Schmelling,¹⁰ B. Schmidt,³⁷ O. Schneider,³⁸

A. Schopper,³⁷ M.-H. Schune,⁷ R. Schwemmer,³⁷ B. Sciascia,¹⁸ A. Sciubba,²⁴ M. Seco,³⁶ A. Semennikov,³⁰ K. Senderowska,²⁶ I. Sepp,⁵² N. Serra,³⁹ J. Serrano,⁶ P. Seyfert,¹¹ M. Shapkin,³⁴ I. Shapoval,^{16,42,e} Y. Shcheglov,²⁹ T. Shears,⁵¹ L. Shekhtman,³³ O. Shevchenko,⁴² V. Shevchenko,³⁰ A. Shires,⁹ R. Silva Coutinho,⁴⁷ M. Sirendi,⁴⁶ N. Skidmore,⁴⁵ T. Skwarnicki,⁵⁸ N. A. Smith,⁵¹ E. Smith,^{54,48} E. Smith,⁵² J. Smith,⁴⁶ M. Smith,⁵³ M. D. Sokoloff,⁵⁶ F. J. P. Soler,⁵⁰ F. Soomro,³⁸ D. Souza,⁴⁵ B. Souza De Paula,² B. Spaan,⁹ A. Sparkes,⁴⁹ P. Spradlin,⁵⁰ F. Stagni,³⁷ S. Stahl,¹¹ O. Steinkamp,³⁹ S. Stevenson,⁵⁴ S. Stoica,²⁸ S. Stone,⁵⁸ B. Storaci,³⁹ M. Straticiuc,²⁸ U. Straumann,³⁹ V. K. Subbiah,³⁷ L. Sun,⁵⁶ W. Sutcliffe,⁵² S. Swientek,⁹ V. Syropoulos,⁴¹ M. Szczekowski,²⁷ P. Szczypka,^{38,37} D. Szilard,² T. Szumlak,²⁶ S. T'Jampens,⁴ M. Teklishyn,⁷ G. Tellarini,^{16,e} E. Teodorescu,²⁸ F. Teubert,³⁷ C. Thomas,⁵⁴ E. Thomas,³⁷ J. van Tilburg,¹¹ V. Tisserand,⁴ M. Tobin,³⁸ S. Tolk,⁴¹ L. Tomassetti,^{16,e} D. Tonelli,³⁷ S. Topp-Joergensen,⁵⁴ N. Torr,⁵⁴ E. Tournefier,^{4,52} S. Tourneur,³⁸ M. T. Tran,³⁸ M. Tresch,³⁹ A. Tsaregorodtsev,⁶ P. Tsopelas,⁴⁰ N. Tuning,^{40,37} M. Ubeda Garcia,³⁷ A. Ukleja,²⁷ A. Ustyuzhanin,^{52,p} U. Uwer,¹¹ V. Vagnoni,¹⁴ G. Valenti,¹⁴ A. Vallier,⁷ R. Vazquez Gomez,¹⁸ P. Vazquez Regueiro,³⁶ C. Vázquez Sierra,³⁶ S. Vecchi,¹⁶ J. J. Velthuis,⁴⁵ M. Veltri,^{17,g} G. Veneziano,³⁸ M. Vesterinen,³⁷ B. Viaud,⁷ D. Vieira,² X. Vilasis-Cardona,^{35,n} A. Vollhardt,³⁹ D. Volyanskyy,¹⁰ D. Voong,⁴⁵ A. Vorobyev,²⁹ V. Vorobyev,³³ C. Voß,⁶⁰ H. Voss,¹⁰ R. Waldi,⁶⁰ C. Wallace,⁴⁷ R. Wallace,¹² S. Wandernoth,¹¹ J. Wang,⁵⁸ D. R. Ward,⁴⁶ N. K. Watson,⁴⁴ A. D. Webber,⁵³ D. Websdale,⁵² M. Whitehead,⁴⁷ J. Wicht,³⁷ J. Wiechczynski,²⁵ D. Wiedner,¹¹ L. Wiggers,⁴⁰ G. Wilkinson,⁵⁴ M. P. Williams,^{47,48} M. Williams,⁵⁵ F. F. Wilson,⁴⁸ J. Wimberley,⁵⁷ J. Wishahi,⁹ W. Wislicki,²⁷ M. Witek,²⁵ G. Wormser,⁷ S. A. Wotton,⁴⁶ S. Wright,⁴⁶ S. Wu,³ K. Wyllie,³⁷ Y. Xie,^{49,37} Z. Xing,⁵⁸ Z. Yang,³ X. Yuan,³ O. Yushchenko,³⁴ M. Zangoli,¹⁴ M. Zavertyaev,^{10,a} F. Zhang,³ L. Zhang,⁵⁸ W. C. Zhang,¹² Y. Zhang,³ A. Zhelezov,¹¹ A. Zhokhov,³⁰ L. Zhong,³ and A. Zvyagin³⁷

(LHCb Collaboration)

¹Centro Brasileiro de Pesquisas Físicas (CBPF), Rio de Janeiro, Brazil

²Universidade Federal do Rio de Janeiro (UFRJ), Rio de Janeiro, Brazil

³Center for High Energy Physics, Tsinghua University, Beijing, China

⁴LAPP, Université de Savoie, CNRS/IN2P3, Annecy-Le-Vieux, France

⁵Clermont Université, Université Blaise Pascal, CNRS/IN2P3, LPC, Clermont-Ferrand, France

⁶CPPM, Aix-Marseille Université, CNRS/IN2P3, Marseille, France

⁷LAL, Université Paris-Sud, CNRS/IN2P3, Orsay, France

⁸LPNHE, Université Pierre et Marie Curie, Université Paris Diderot, CNRS/IN2P3, Paris, France

⁹Fakultät Physik, Technische Universität Dortmund, Dortmund, Germany

¹⁰Max-Planck-Institut für Kernphysik (MPIK), Heidelberg, Germany

¹¹Physikalisches Institut, Ruprecht-Karls-Universität Heidelberg, Heidelberg, Germany

¹²School of Physics, University College Dublin, Dublin, Ireland

¹³Sezione INFN di Bari, Bari, Italy

¹⁴Sezione INFN di Bologna, Bologna, Italy

¹⁵Sezione INFN di Cagliari, Cagliari, Italy

¹⁶Sezione INFN di Ferrara, Ferrara, Italy

¹⁷Sezione INFN di Firenze, Firenze, Italy

¹⁸Laboratori Nazionali dell'INFN di Frascati, Frascati, Italy

¹⁹Sezione INFN di Genova, Genova, Italy

²⁰Sezione INFN di Milano Bicocca, Milano, Italy

²¹Sezione INFN di Padova, Padova, Italy

²²Sezione INFN di Pisa, Pisa, Italy

²³Sezione INFN di Roma Tor Vergata, Roma, Italy

²⁴Sezione INFN di Roma La Sapienza, Roma, Italy

²⁵Henryk Niewodniczanski Institute of Nuclear Physics Polish Academy of Sciences, Kraków, Poland

²⁶Faculty of Physics and Applied Computer Science, AGH—University of Science and Technology, Kraków, Poland

²⁷National Center for Nuclear Research (NCBJ), Warsaw, Poland

²⁸Horia Hulubei National Institute of Physics and Nuclear Engineering, Bucharest-Magurele, Romania

²⁹Petersburg Nuclear Physics Institute (PNPI), Gatchina, Russia

³⁰Institute of Theoretical and Experimental Physics (ITEP), Moscow, Russia

³¹Institute of Nuclear Physics, Moscow State University (SINP MSU), Moscow, Russia

³²Institute for Nuclear Research of the Russian Academy of Sciences (INR RAN), Moscow, Russia

³³Budker Institute of Nuclear Physics (SB RAS) and Novosibirsk State University, Novosibirsk, Russia

- ³⁴*Institute for High Energy Physics (IHEP), Protvino, Russia*
- ³⁵*Universitat de Barcelona, Barcelona, Spain*
- ³⁶*Universidad de Santiago de Compostela, Santiago de Compostela, Spain*
- ³⁷*European Organization for Nuclear Research (CERN), Geneva, Switzerland*
- ³⁸*Ecole Polytechnique Fédérale de Lausanne (EPFL), Lausanne, Switzerland*
- ³⁹*Physik-Institut, Universität Zürich, Zürich, Switzerland*
- ⁴⁰*Nikhef National Institute for Subatomic Physics, Amsterdam, The Netherlands*
- ⁴¹*Nikhef National Institute for Subatomic Physics and VU University Amsterdam, Amsterdam, The Netherlands*
- ⁴²*NSC Kharkiv Institute of Physics and Technology (NSC KIPT), Kharkiv, Ukraine*
- ⁴³*Institute for Nuclear Research of the National Academy of Sciences (KINR), Kyiv, Ukraine*
- ⁴⁴*University of Birmingham, Birmingham, United Kingdom*
- ⁴⁵*H.H. Wills Physics Laboratory, University of Bristol, Bristol, United Kingdom*
- ⁴⁶*Cavendish Laboratory, University of Cambridge, Cambridge, United Kingdom*
- ⁴⁷*Department of Physics, University of Warwick, Coventry, United Kingdom*
- ⁴⁸*STFC Rutherford Appleton Laboratory, Didcot, United Kingdom*
- ⁴⁹*School of Physics and Astronomy, University of Edinburgh, Edinburgh, United Kingdom*
- ⁵⁰*School of Physics and Astronomy, University of Glasgow, Glasgow, United Kingdom*
- ⁵¹*Oliver Lodge Laboratory, University of Liverpool, Liverpool, United Kingdom*
- ⁵²*Imperial College London, London, United Kingdom*
- ⁵³*School of Physics and Astronomy, University of Manchester, Manchester, United Kingdom*
- ⁵⁴*Department of Physics, University of Oxford, Oxford, United Kingdom*
- ⁵⁵*Massachusetts Institute of Technology, Cambridge, Massachusetts, USA*
- ⁵⁶*University of Cincinnati, Cincinnati, Ohio, USA*
- ⁵⁷*University of Maryland, College Park, Maryland, USA*
- ⁵⁸*Syracuse University, Syracuse, New York, USA*
- ⁵⁹*Pontifícia Universidade Católica do Rio de Janeiro (PUC-Rio), Rio de Janeiro, Brazil, associated with Universidade Federal do Rio de Janeiro (UFRJ), Rio de Janeiro, Brazil*
- ⁶⁰*Institut für Physik, Universität Rostock, Rostock, Germany, associated with Physikalisches Institut, Ruprecht-Karls-Universität Heidelberg, Heidelberg, Germany*
- ⁶¹*KVI-University of Groningen, Groningen, The Netherlands, associated with Nikhef National Institute for Subatomic Physics, Amsterdam, The Netherlands*
- ⁶²*Celal Bayar University, Manisa, Turkey, associated with European Organization for Nuclear Research (CERN), Geneva, Switzerland*

^aAlso at P.N. Lebedev Physical Institute, Russian Academy of Science (LPI RAS), Moscow, Russia.

^bAlso at Università di Bari, Bari, Italy.

^cAlso at Università di Bologna, Bologna, Italy.

^dAlso at Università di Cagliari, Cagliari, Italy.

^eAlso at Università di Ferrara, Ferrara, Italy.

^fAlso at Università di Firenze, Firenze, Italy.

^gAlso at Università di Urbino, Urbino, Italy.

^hAlso at Università di Modena e Reggio Emilia, Modena, Italy.

ⁱAlso at Università di Genova, Genova, Italy.

^jAlso at Università di Milano Bicocca, Milano, Italy.

^kAlso at Università di Roma Tor Vergata, Roma, Italy.

^lAlso at Università di Roma La Sapienza, Roma, Italy.

^mAlso at Università della Basilicata, Potenza, Italy.

ⁿAlso at LIFAELS, La Salle, Universitat Ramon Llull, Barcelona, Spain.

^oAlso at Hanoi University of Science, Hanoi, Viet Nam.

^pAlso at Institute of Physics and Technology, Moscow, Russia.

^qAlso at Università di Padova, Padova, Italy.

^rAlso at Università di Pisa, Pisa, Italy.

^sAlso at Scuola Normale Superiore, Pisa, Italy.